Journal of Robotics and Control (JRC)
Volume 5, Issue 5, 2024
ISSN: 2715-5072, DOI: 10.18196/jrc.v5i5.22118

Performance Optimization of a DFIG-based Variable Speed Wind Turbines by IVC-ANFIS Controller

Said Ouhssain [1], Hamid Chojaa [2], Yahya Aljarhizi [3], Elmehdi Al Ibrahmi [4], Aziz Hadoune [5], Alfian Ma'arif [6], Iswanto Suwarno [7], Mahmoud A. Mossa [8*]
[1, 3, 4] Laboratory of Materials Physics and Subatomic, Ibn Tofaïl University, Faculty of Sciences, Kénitra-14000, Morocco
[2] Higher School of Technology, Industrial Technologies and Services Laboratory, Sidi Mohamed Ben Abdellah University, Fez 30000, Morocco
[5] Energy, Materials and Computing Physics Research Group, ENS, Abdelmalek Essaadi University, Tetouan 93020, Morocco
[6] Department of Electrical Engineering, Universitas Ahmad Dahlan, Yogyakarta, Indonesia
[7] Department of Electrical Engineering, Universitas Muhammadiyah Yogyakarta, Yogyakarta, Indonesia
[8] Electrical Engineering Department, Faculty of Engineering, Minia University, Minia 61111, Egypt.
Emails: [1] said.ouhssain@uit.ac.ma, [2] hamid.chojaa@usmba.ac.ma, [3] yahya.m.ymn@gmail.com, [4] alibrahmielmehdi@yahoo.fr, [5] aziz.hadoun@etu.uae.ac.ma, [6] alfianmaarif@ee.uad.ac.id, [7] iswanto_te@umy.ac.id, [8] mahmoud_a_mossa@mu.edu.eg
*Corresponding Author

***Abstract*—An improved indirect vector control (IVC) method for a wind energy conversion system (WECS) is presented in this research. Field-oriented control or indirect vector control as it is sometimes called is a very important element of contemporary WECS that employs DFIGs. This control strategy is pivotal for achieving high performance and efficiency of DFIG-based wind turbines because it offers direct control on the torque and power ratings of the generator. A doubly fed induction generator (DFIG) is used by the WECS to inject power to the grid. An adaptive network-based fuzzy inference system (ANFIS), which is proposed to replace traditional methods like linear PI controllers, is the basis for this IVC. In this paper we chose ANFIS controller over traditional linear Proportional-Integral (PI) controllers due to its ability to adapt and learn from the system, leading to improved performance. The rotor voltage is controlled by the proposed IVC in order to regulate the exchanged active and reactive power between the stator and the grid. In order to verify the proposed control in terms of performance and robustness, a comparative analysis between the proposed ANFIS and linear PI controllers for the WECS-DFIG system is performed by a simulation study in a MATLAB/Simulink environment. This analysis covers both the transient and steady states of operation. As a result, the proposed ANFIS controller shows improved efficiency and robustness compared to the linear PI controllers. This superiority stems from its ability to integrate the flexibility and effectiveness inherent in diverse artificial intelligence controllers, specifically the synergistic use of Neural Network (NN) and Fuzzy Logic (FL) algorithms. The ANFIS controller's adaptability to diverse operating conditions and its capability to learn and optimize its performance play pivotal roles in enhancing its control capabilities within the WECS-DFIG system.**

***Keywords*—Wind Energy; Double-Fed Induction Generator; WECS; Indirect Vector Control; Artificial Intelligence Controller; ANFIS.**

I. INTRODUCTION

Distributed generation and renewable energy sources, such as wind and solar power, have garnered significant interest as a potential substitute to fulfill the world's energy requirements [1]. Wind power has gained global recognition due to two primary factors: the escalating costs associated with fossil fuels and the pressing need to curb CO2 emissions [2]. One of the most significant renewable energy sources today is wind energy, which is predicted to produce 2110 GW of power globally by 2030, accounting for up to 20% of global electricity consumption [3]. Wind energy sources are required to participate in electricity markets in many countries [4].

Variable-speed wind turbines are the most recent generation. The functioning of this type lowers mechanical stress, boosts energy efficiency, and enhances the caliber of electrical energy produced [5]. With its exceptional advantages, like large-scale production with decreased static converter losses and flexibility in operation, the variable-speed wind tur-bine with a DFIG is the most widely used wind turbine technology available today. Moreover, it has the capacity to minimize mechanical stress on the turbine, regulate the flow of power, and enable fault ride-through [6]. A number of studies, including [7]-[10], have provided different DFIG control strategies for wind turbines.

The unpredictability of wind patterns adds extra difficulty to the design of grid-integrated wind energy conversion systems (WECS). The fluctuating and ever-changing characteristics of wind present a significant obstacle to attaining steady and effective management of the energy conversion procedure. In the past, WECS has used traditional control techniques, such as conventional and linear controllers. However, their limitations in terms of efficiency and performance have prompted the exploration of alternative control strategies [11]. Concerning energy trading according to the time of day, taking into account the different levels of uncertainty in production and price throughout the day, it is important to minimize costs by introducing new ordering strategies that are cheaper than the traditional strategies [12]-[13]. Some control strategies are more effective and efficient than others. Vector control is one of

the most widely used methods for controlling electric machines.

In industrial applications, vector control is a common method for controlling induction machines due to its high dynamic performance for controlling the speed and torque of AC machines [14]. In actuality, managing the power exchanges particularly the active and reactive power supplied to the grid is a necessary part of managing the DFIG through the vector control approach. These controllers consequently exhibit high response times, overshoot, and transient and steady-state faults [15]. Direct and indirect vector controls (IVC), also known as field-oriented control (FOC), are the two types of vector control. PI controllers are frequently used in FOC to provide nonlinear control of active and reactive power in WECS that is based on DFIG [16]-[17]. Nonetheless, the IVC is a more useful and effective approach because it determines the rotor position based on the motor's speed feedback signal. When compared to direct vector control, this vector control provides superior dynamic performance overall [18].

The present study aims to use an Adaptive Neuro-Fuzzy Inference System (ANFIS) controller to construct an intelligent Indirect Vector Control (IVC) approach for a wind-driven DFIG. Artificial neural networks (ANNs) and fuzzy logic systems are combined in ANFIS, a technology that is widely used in artificial intelligence, machine learning, and control systems [19]. The proposed model ANFIS also known as Adaptive Neuro-Fuzzy Inference System applies the integration of neural networks and fuzzy logic for an efficient control of Wind Energy Conversion Systems abbreviated WECS. Hence the ability of ANFIS to learn nonlinear relationships between input data and predict output values makes it optimize power production by responding to the dynamic parameters such as output voltage. This integration of fuzzy logic and neural networks make ANFIS more suitable for such systems because it can cope up with the dynamic behavior of the wind turbine systems which is very unpredictable in nature than any other method provides more efficient and less costly solution to the enhancement of the energy production [20]. Real time learning capability of the system in finding the required control parameters for WECS yield better performances and flexibility of its control strategies with regard to fluctuations in wind speeds and conditions. The indirect vector control strategy architecture based on the adaptive network-based fuzzy inference system (ANFIS) has the remarkable feature of rapid convergence while integrating the flexibility of fuzzy logic with the suppleness of neural networks [21]. Overall, ANFIS optimizes controller performance by providing better control of load and wind speed variations in WECS using DFIGs.

The hybrid model exhibits efficacy in simulating intricate and nonlinear correlations between input and output data, making it especially fitting for tackling the dynamic and unpredictable characteristics of wind turbine systems. To put it briefly, the ANFIS controller advances intelligent control systems in renewable energy applications by utilizing fuzzy logic's interpretability and ANNs' learning capabilities to improve DFIG control precision.

The wind turbine power system's dynamic reaction is enhanced following a fault with the usage of the ANFIS controller [22]. Its purpose is to maximize torque and regulate voltage when there are wind turbines and other disturbances. Via utilizing an appropriate learning technique based on the error equation, the ANFIS controller modifies the neural network's parameters. High precision, minimal oscillation, and ripple have been demonstrated in the suggested ANFIS controller's ability to maintain optimal performances under a variety of disturbances. It effectively stabilizes the system quickly, making it a suitable choice for controlling power systems of wind turbines [23].

The proposed ANFIS-based approach in DFIG-based wind energy systems has significantly improved control precision, enhanced system stability, and optimized overall energy conversion efficiency. ANFIS, which integrates fuzzy logic control and artificial neural networks, offers a reliable control method for systems where exact mathematical modeling is complex or impractical [24].

An improved ANFIS-based direct torque and flux control scheme has demonstrated better dynamic performance and more precise control of electromechanical torque and stator current across various wind speeds, outperforming basic fuzzy logic and conventional PI controllers [25].

Furthermore, the ANFIS controller plays a crucial role in maintaining output voltage stability and consistent supply frequency in grid-connected DFIG-based wind energy systems, even under varying load conditions and turbulent wind speeds [26].

The paper is structured as follows: In Sec. 2, the wind energy conversion system's dynamic model is displayed. This includes modeling the WECS, notably the lumped model of the wind turbine, as well as modeling the DFIG. In Sec. 3, the objectives of setup and control are discussed. In Sec. 4, the implemented control strategies are explained. In Sec. 5, the simulated results of the two control approaches are introduced and discussed using the real wind profile of El Hocima, Morocco. A conclusion and some ideas are presented in Section 6, highlighting the importance of intelligent IVC for improving the efficiency and dependability of DFIG-based wind energy systems. Description and modeling of the pro-posed system.

The proposed WECS's general structure is depicted in Fig. 1. An IVC controller using an adaptive network-based fuzzy inference system (ANFIS) governs the rotor of a grid-connected DFIG in this system. A rotor-side converter (RSC) connected to a grid-side converter (GSC) is being managed by the controller.

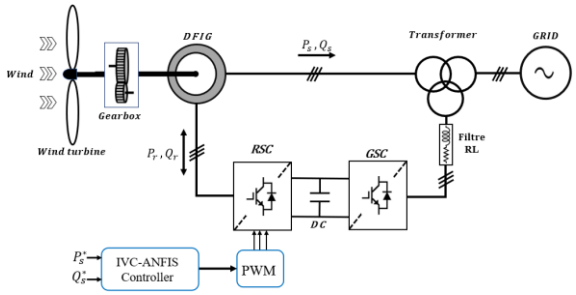

Fig. 1. Proposed WECS based on a grid-connected DFIG

II. DESCRIPTION AND MODELING OF THE PROPOSED SYSTEM

A. Modeling of Wind Turbine

In order to transform wind energy into electrical energy, a turbine was created in the last century. Wind energy is transformed into mechanical energy and used to drive an electric generator [23]-[25]. Although wind turbines can have two or three blades, three-bladed wind turbines are the most widely utilized on both land and water [26]. Equations can be used to express the power and torque generated by a wind turbine [27]:

$$P_t = C_p P_w = \frac{1}{2} C_p(\lambda, \beta) \rho S v^3 \quad (1)$$

$$T_{aer} = \frac{1}{2\Omega_t} \rho \pi R^2 V^3 C_P(\lambda, \beta) \quad (2)$$

The power coefficient (C_p), an important factor, is used to calculate the wind turbine power. The value of C_p, which is influenced by the angle at which the turbine blades interact the wind, has a maximum value of 0.59. The value of C_p can be mathematically evaluated by:

$$C_p(\lambda, \beta) = 0.5\left(\frac{116}{\lambda_i} - 0.4\beta - 5\right) exp\left(\frac{-21}{\lambda_i}\right) + 0.0068\lambda \quad (3)$$

A crucial parameter of a wind turbine that determines the highest power rate that can be drawn from the wind is the tip speed ratio (TSR). It holds equal significance to the power coefficient. The wind turbine being studied in the paper has a specific TSR, which is described by (5).

$$\frac{1}{\lambda_i} = \frac{1}{\lambda + 0.08\beta} - \frac{0.035}{\beta^3 + 1} \quad (4)$$

$$\lambda = \frac{\omega_t R}{V} \quad (5)$$

where ω_t is the turbine speed, β is the blade pitch angle (in degrees), and λ is the tip-speed-ratio.

The graphical representation of (3) is illustrated in Fig. 2. The Fig. 2 shows that the maximum value of $C_p(\lambda, \beta)$ is 0.4798, which occurs when β is 0° and λ_{opt} is 8.124.

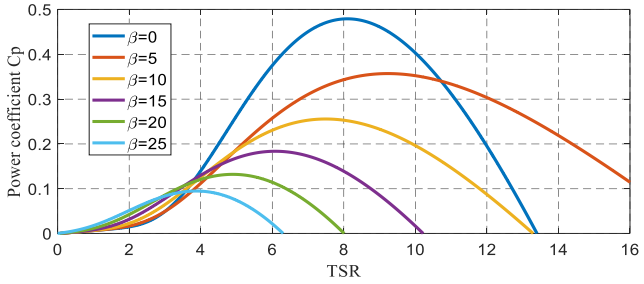

Fig. 2. Graphical illustration of relationship (3)

Formulation (6) explains how the torque and speed of the electric generator and turbine are related to each other. It shows that the turbine has a greater torque compared to the electric generator, but the electric generator has a higher speed than the turbine.

$$\begin{cases} T_m = \dfrac{T_{aer}}{G} \\ \omega_m = G\omega_t \end{cases} \quad (6)$$

where ω_t is the turbine speed, G is the gearbox ratio, Taer is the aerodynamic torque.

The mechanical part of the turbine-generator system is illustrated by equation (7), which also establishes how the electric machine operates as an electric generator or as a motor.

$$J\frac{d\omega_m}{dt} = T_m - T_g - C_f \quad (7)$$

where ω_m is the generator's mechanical speed, T_m is the shaft torque, T_g is the developed generator's torque.

B. Modeling of DFIG

The dynamic equations for the voltages, fluxes, and active and reactive powers of the DFIG in the reference d-q park are given by the following formulas [28].

The stator voltages are given by:

$$\begin{cases} V_{ds} = R_s I_{ds} + \dfrac{d\phi_{ds}}{dt} - \phi_{qs}\omega_s \\ V_{qs} = R_s I_{qs} + \dfrac{d\phi_{qs}}{dt} + \phi_{ds}\omega_s \end{cases} \quad (8)$$

The rotor voltages are given by:

$$\begin{cases} V_{dr} = R_r I_{dr} + \dfrac{d\phi_{dr}}{dt} - \phi_{qr}(\omega_s - \omega_r) \\ V_{qr} = R_r I_{qr} + \dfrac{d\phi_{qr}}{dt} + \phi_{dr}(\omega_s - \omega_r) \end{cases} \quad (9)$$

The developed torque is evaluated by:

$$T_g = \frac{3}{2} p L_m (I_{qs} I_{dr} - I_{ds} I_{qr}) \quad (10)$$

With, V_{ds}, V_{qs}, V_{dr} and V_{qr} are the d-q components of stator and rotor voltages, in turns. I_{ds}, I_{qs}, I_{dr} and I_{qr} are the d-q components of stator and rotor currents, respectively. φ_{ds}, φ_{qs}, φ_{dr} and φ_{qr} are the d-q parts of stator and rotor fluxes, respectively. Where L_s, L_r, R_s, and R_r stand for the inductances and winding resistances of the rotor and stator, respectively. L_m is the magnetizing inductance. ω_s, ω_r are the angular frequencies of the stator and rotor, p is the DFIG's pole pairs.

III. PROPOSED CONTROL STRATEGY

A. Flux Orientation Technique

Field-Oriented Control (FOC) or vector control is selected due to its capacity to allow the mannered and optimum control of motor speed and torque, whereby the stator current is divided to segments that produce the torque and flux, respectively [5]. This technique uses a technique to transform the 3-phase AC voltage and current signals into a rotating reference frame to control the flow of stator currents and segregate them in to torque and flux components. Through implementing the PI controller, the Park inverse transform flux orientation method helps in generating the control signals of the motor drive depending on the torque and flux values to be attained, thus supporting

the managerial and organizational goal of efficient and valid operational control of induction motors in different applications [6]. Also, other measures such as the loss reduction controllers and the new vector control techniques improve the performance and efficiency of induction motor drives, especially in applications like electric vehicles where energy management is a critical factor. In this paper, vector control approach using the stator flux orientation is used. Along the direct axis, the field is orientated and rotated. The d-q axis alignment to the stator flux is shown in Fig. 3.

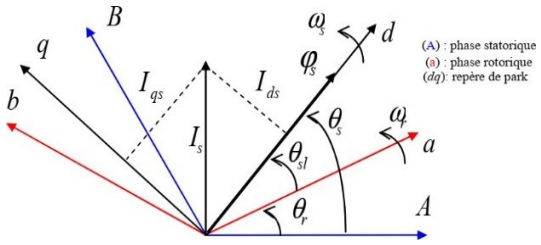

Fig. 3. d-q axis orientation to the stator flux

Then we have: $\Phi_{ds}=\Phi_s$ and $\Phi_{qs}=0$. Therefore, the developed torque of (10) then becomes:

$$T_g = -\frac{3}{2}pL_m(I_{ds}I_{qr}) \tag{11}$$

This selection is not made randomly. This is supported by the fact that the generator is frequently connected to a high-power network with steady voltage and frequency, which results in a stator flux statement for the DFIG. For high power machines, it is typical to assume that the stator winding resistance is ignored [29]. However, the system of (8) can be simplified as follows:

$$\begin{aligned} V_{ds} &= 0 \\ V_{qs} &= V_s = \phi_s\omega_s \end{aligned} \tag{12}$$

The stator active and reactive powers are calculated by:

$$\begin{cases} P_s = \frac{3}{2}(V_{ds}I_{ds} + V_{qs}I_{qs}) \\ Q_s = \frac{3}{2}(V_{qs}I_{ds} - V_{ds}I_{qs}) \end{cases} \tag{13}$$

From (12) and (13), we obtain:

$$\begin{cases} P_s = \frac{3}{2}V_sI_{qs} \\ Q_s = \frac{3}{2}V_sI_{ds} \end{cases} \tag{14}$$

Stator currents are given by:

$$\begin{cases} I_{ds} = \dfrac{\phi_s - L_mI_{dr}}{L_s} \\ I_{qs} = \dfrac{L_m}{L_s}I_{qr} \end{cases} \tag{15}$$

The rotor voltages are obtained by substituting equation (15) with (9).

$$\begin{cases} V_{dr} = R_rI_{dr} + \sigma L_r\dfrac{dI_{dr}}{dt} - \omega_s\, g\sigma L_rI_{qr} \\ V_{qr} = R_rI_{qr} + \sigma L_r\dfrac{dI_{qr}}{dt} + \omega_s\, g\sigma L_rI_{dr} + g\dfrac{M}{L_s}V_s \end{cases} \tag{16}$$

All these equations are the main pillars of the Block diagram of the simplified model of the DFIG shown in Fig. 4.

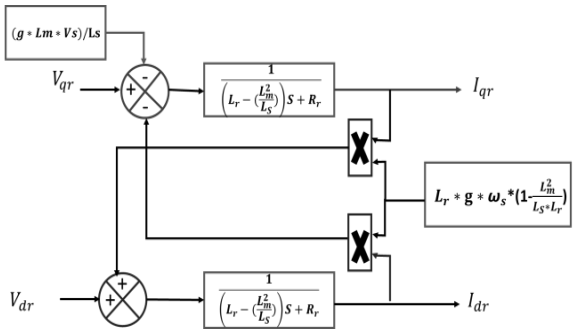

Fig. 4. Block diagram of the simplified model of the DFIG

B. *Decoupled Control of Active and Reactive Powers Using ANFIS Controller*

To manage the rotor powers and currents, an independent control system is implemented that takes into account the coupling factors and compensates for them [30]. This method is called indirect method. It introduces techniques of artificial intelligence; in this article we use the technique of Neuro-Flow (ANFIS). A neural fuzzy network is a hybrid artificial intelligence system that combines fuzzy logic and artificial neural networks to infer fuzzy set and fuzzy rule parameters from data. The desired network is constructed using MATLAB's ANFIS toolbox, and all data is gathered into a unique matrix. Because the neural network has a great capacity for learning and the fuzzy system offers good knowledge, the benefits of merging these two complimentary techniques into one system improve the overall performance, which is known as the neuro-fuzzy system [31]. On the other hand, when fuzzy rules are injected into a neural network, the initialization of the network parameters becomes stable and obvious. As a result, the computation time needed for the identification is much decreased.

Fig. 5 shows the representation of the DFIG using the indirect vector control scheme. Four controllers are used to control the power, torque and field current. In the present work, these controllers are ANFIS type fuzzy logic controllers. The inverter used to control both the voltage and frequency of the voltage applied to the motor is controlled using the space vector pulse width modulation method.

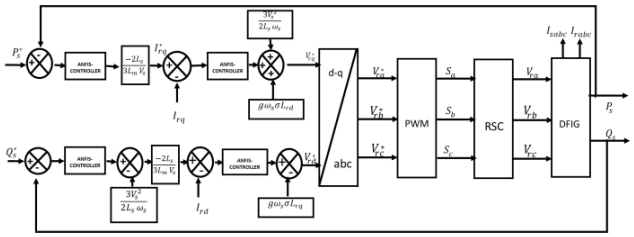

Fig. 5. The proposed indirect vector control bloc diagram using the (Adaptive Network Based Fuzzy Inference System) ANFIS

IV. ANFIS MODEL

A. *ANFIS Architecture*

The neuro-fuzzy adaptive inference system (ANFIS) under study makes use of a 5-layer MLP neural network. In a Takagi-Sugeno fuzzy inference system, each layer represents the realization of a single step. For the sake of simplicity, we

will assume that the fuzzy inference system has two inputs (x and y) and an output (f). Furthermore, presuming that there are two Takagi-Sugeno fuzzy rules in the rule base [32].

Rule1: If x is A1 and y is B1 THEN

$$f1 = p1\,x + q1\,y + r1 \tag{17}$$

Rule 2: If x is A2 and y is B2 THEN

$$f2 = p2\,x + q2\,y + r2 \tag{18}$$

Fig. 6 illustrates the five-layer architecture of the ANFIS.

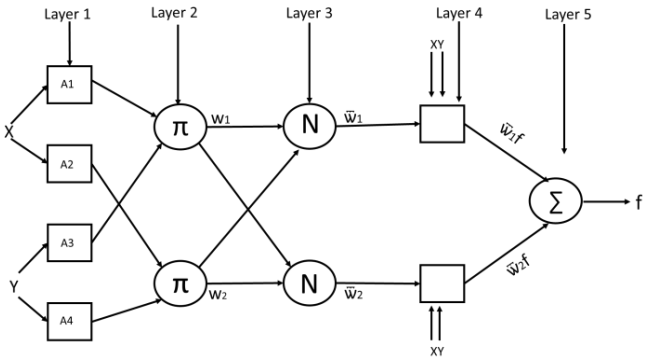

Fig. 6. Architecture of ANFIS controllers

The number of neurons in the first layer of the ANFIS architecture in this design is equal to the number of fuzzy subsets in the inference system that is being studied. Every neuron uses its transfer function to determine how true a given fuzzy subset is. The requirement that it be derivable is the only limitation on the selection of this transfer function. As in the literature, the operational and modifiable parameters of the Gaussian function are the center and the gradient of the Gaussian function [33]. The following represents the activation function of first layer neuron (i):

$$f_i^1 = \mu A_i(x) \tag{19}$$

where A_i is a fuzzy subset that corresponds to the variable x, and x is the input to neuron i. Stated differently, it represents the degree to which a given x satisfies A_i and serves as the membership function of A_i. Since we select $\mu A_i(x)$ to be either trapezoidal, Gaussian, or triangular with a minimum of 0 and a maximum of 1, the generalized functions of the triangle and Gaussian forms are displayed in (20) and (21), respectively [34].

$$\mu(x) = max\left(min\left(\frac{x-a}{b-a}, \frac{c-x}{c-b}\right), 0\right) \tag{20}$$

$$\mu(x) = exp\left(-\frac{(x-a)2}{\sigma^2}\right) \tag{21}$$

The collection of parameters, denoted as $\{a, b, c, \sigma\}$, represent distinct variants of the language variable $A_i's$ membership function. Changes in the values of these parameters are accompanied by changes in the function of the previous form. The parameters of the membership function are the ones found in this layer.

In contrast, the second hidden layer of the ANFIS architecture is used to determine the premises' level of activation. This layer consists of neurons that represent each rule premise. These neurons are in charge of calculating the degree of truth of each premise and receiving as input the degree of truth of the various fuzzy subsets that comprise it. These neurons' activation functions are determined by the operators (AND or OR) included in the rules. The first layer's neurons i activation function can be stated as follows:

$$W_k = \mu A_i(x) \times \mu A_i(y) \tag{22}$$

where i denotes the number of x partitions, j the number of y partitions, and k the number of rules.

The rule weight normalization corresponds to the third layer, the ratio between the rule weight i and the total of all rule weights is calculated.

$$\bar{w}_k = \frac{\mathrm{w_k}}{\sum w} \tag{23}$$

This layer output is called the normalized weights. For the fourth layer, each node i in this layer is a node evaluated by

$$f_k^4 = \bar{w}_k \times f_k = \bar{w}_k x(p_k x + q_k y + r) \tag{24}$$

where $\{p_i, q_i, r_i\}$ is the set of parameters and $\bar{w}_k$ is the third layer's output. We refer to these parameters as the subsequent parameters.

The inputs and outputs from the preceding layer are integrated in the output layer, which is the fifth layer. As a result, the single node is a constant node, and the total outcome is obtained by summarizing the signal set that follows:

$$f^5 = \sum_k \bar{w}_k x\, f_k^4 \tag{25}$$

The decision unit, fuzzification interface, database, rule base, and defuzzification interface are the five functional components that make up the ANFIS structure [35]. The neuro-fuzzy system that was built is a Sugeno system of first order with a single input and seven distribution membership functions. Seven if-then rules comprise it. Fig. 7 shows the basic architecture of the created neuro-fuzzy system with the error signal of the controlled variable, i.e., active or reactive power or current, as input.

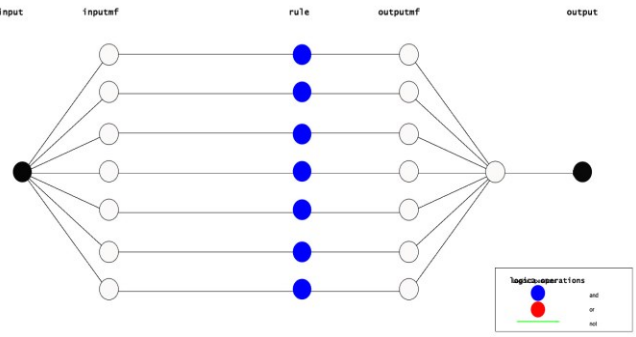

Fig. 7. Internal structure of the proposed ANFIS controller

The learning process makes use of the hybrid backpropagation method. As a result, the training data that is utilized comes from comprehensive vector controller simulations. Additionally, Fig. 8 displays the input membership functions for the active and reactive power controllers.

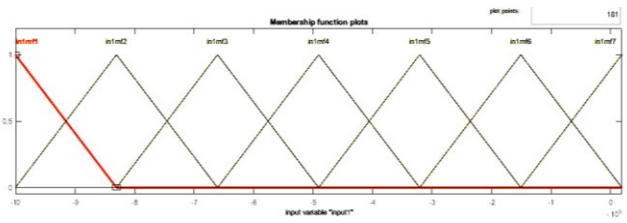

Fig. 8. Input membership functions for active and reactive power controllers

Based on the input membership functions Fig. 9 illustrates the Neuro-Fuzzy learning error for the power controller.

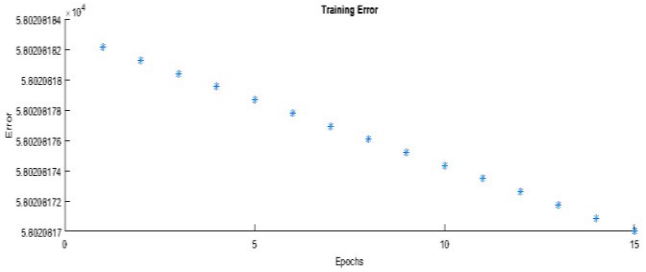

Fig. 9. Neuro-Fuzzy learning error for the power controller

V. EVALUATION RESULTS

A thorough simulation research was carried out to test the proposed IVC technique using the DFIG and adaptive network-based fuzzy inference system (ANFIS) for the wind energy conversion system (WECS). The simulation involved the utilization of two distinct wind profiles: step and random wind. This section of the paper is dedicated to presenting and analyzing the simulation results, with a particular focus on the performance of the ANFIS controller in response to these two wind profiles. The discussion unfolds in two parts, firstly highlighting the outcomes obtained under step wind conditions and subsequently delving into the implications of employing random wind profiles. Through this exploration, a nuanced understanding of the controller's effectiveness and adaptability to diverse wind scenarios is tested.

Table I lists the DFIG and wind turbine's specifications. A comparative study is conducted between two control systems, namely IVC-ANFIS and IVC-PI, concerning the reference track, power ripple, stator current's harmonics and system robustness. This portion of the work also takes into account the robustness to changes in the DFIG parameter and the harmonic distortion of the stator current.

TABLE I. SPECIFICATIONS OF WIND GENERATION SYSTEM

Parameters	Value	Parameters	Value
Blades	3	I_{rn}	8.5 A
Rotor radius R	1 m	Pole pairs, p	2
Gearbox ratio G	3	f_s	50 Hz
f	0.0027 (N.m.s/rad)	R_s	1.18 Ω
J	0.04 kg.m²	R_r	1.66 Ω
P_n	1.5 KW	L_s	0.20 H
V_s	220 / 380 V	L_r	0.18 H
I_{sn}	5.2 A	L_m	0.17 H

A. Insights from Step Wind Simulation

The simulation study is the main focus of the analysis of the proposed IVC method using an adaptive network-based fuzzy inference system (ANFIS) for a WECS-DFIG system.

It reveals the effectiveness of the controller in response to the step wind profiles shown in Fig. 10.

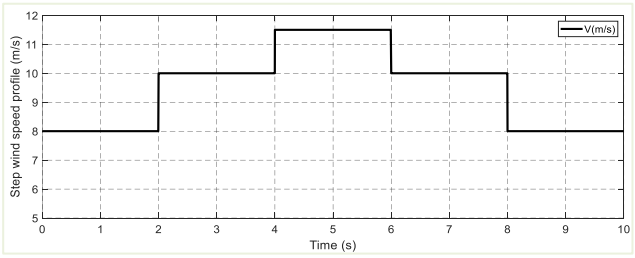

Fig. 10. Wind profiles

The rotor speed is shown in Fig. 11, which clarifies how step wind affects the system's rotational behaviour. This plot provides a good illustration of the rotor speed's response under the ANFIS control method by capturing the dynamic nature of the speed over time.

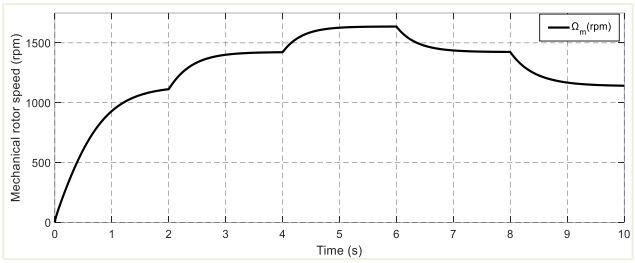

Fig. 11. Mechanical rotor speed (rpm) under step wind

Upon examining Fig. 12(a) and Fig. 12(b), it is evident that there is a notable convergence towards the reference values for both reactive and active power. It's interesting to note that the harvested active power, which can range from 500W to 1400W, can fluctuate greatly with even a slight change in wind speed. It is obvious that active power generation rises with increasing wind speed and falls with decreasing wind speed. Even in the event that wind speed fluctuates, a constant unity power factor is ensured on the network side by maintaining the reference value of reactive power at zero.

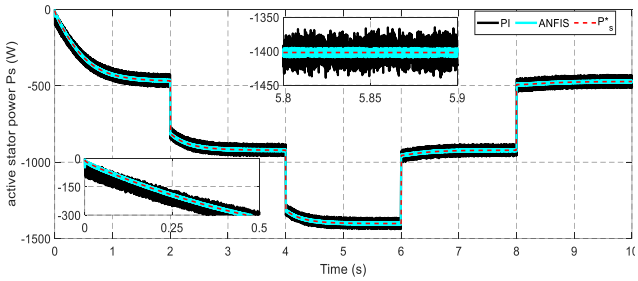

(a) Active power

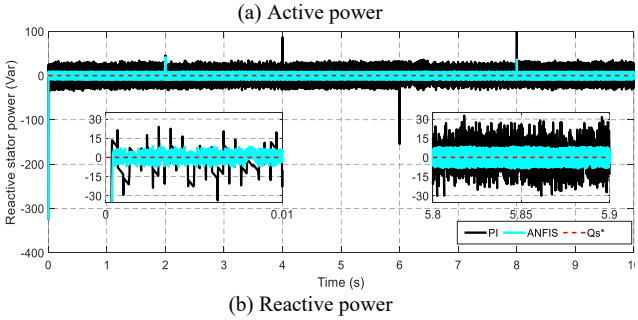

(b) Reactive power

Fig. 12. (a) Active power. (b) Reactive power

The relationship between stator currents, rotor currents, and the applied wind speed profile is highlighted in Fig. 13(a), (b), (c), and (d), demonstrating a measurable association between these three variables. The Fig.s clearly illustrate how wind variations impact the stator and rotor current magnitudes. Remarkably, the currents peak at 3 A, which denotes the highest possible power flow in the system. This reliance on the wind profile emphasises the critical role that outside environmental factors play in figuring out how the system acts.

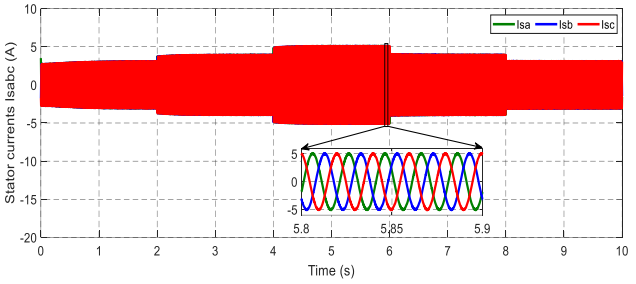

(a) Stator I_{sabc} observed under the PI case of step wind

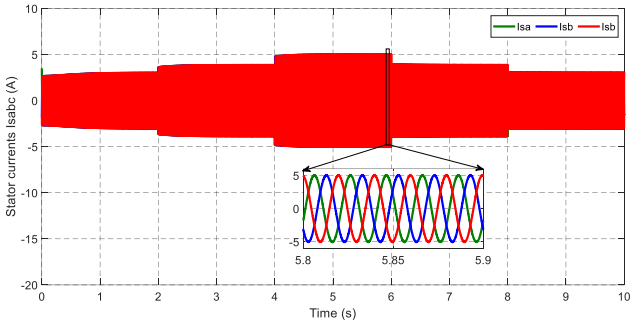

(b) Stator I_{sabc} observed under the ANFIS case of step wind

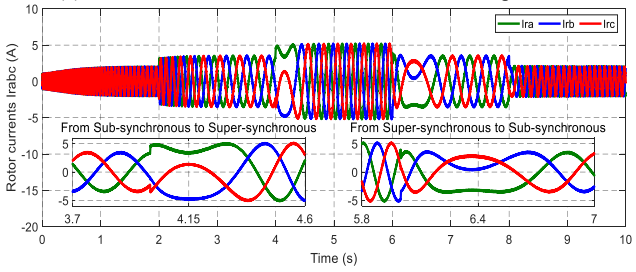

(c) Rotor I_{rabc} observed under the PI case of step wind

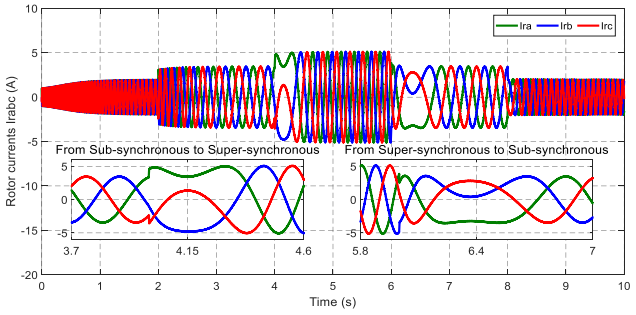

(d) Rotor I_{rabc} observed under the ANFIS case of step wind

Fig. 13. Stator and Rotor currents PI and ANFIS controllers case step wind

In Fig. 14, the system's power factor is visually depicted, indicating an approximate value of 0.98. The graphical representation reveals distinct undulations, directly associated with the operational dynamics and variations in wind speed

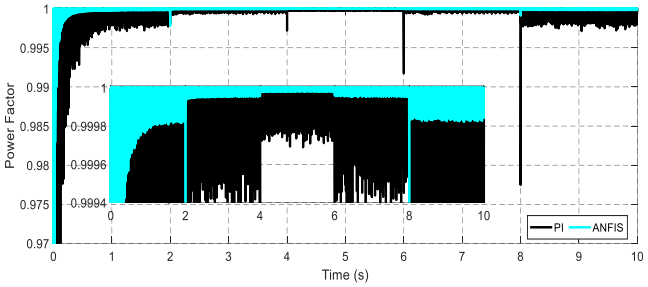

Fig. 14. Power Factor case step wind test

The results of the FFT (Fast Fourier Transform) studies of the generated stator are shown in Fig. 15. The following are the main factors that we took into account:

- Sampling Rate (Fs): To prevent aliasing, the sampling rate is double the maximum frequency.
- Window Function: Before running the FFT on the time-domain signal, the window function Hamming is applied.
- Window Length (N): The number of data points that are used in each FFT computation is known as the window length.
- Overlap: 50%.
- Zero Padding: The time domain signal was terminated before running the FFT
- Averaging: To lessen the impact of noise, multiple FFTs are averaged.
- Window Scaling: To adjust for amplitude loss caused by windowing, a scaling factor of 1.5 was employed.
- Handling of DC Component: Eliminate the DC (0 Hz) component from the FFT results.
- Normalization: Power spectral density measurements were obtained by normalizing the FFT results.

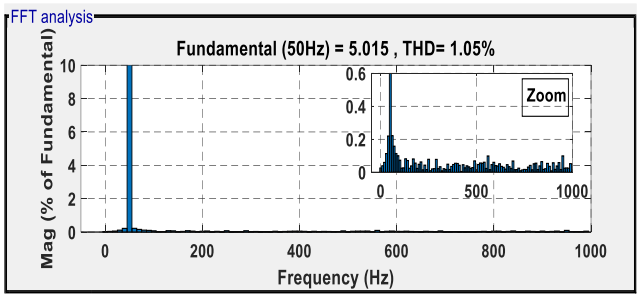

Fig. 15. THD of the current induced utilizing the two controllers under step wind test improved net

B. Evaluating ANFIS Performance under Random Wind Profiles

The wind profile used to test our model is based on wind data recorded in Al Hoceima, Morocco, for a duration of 10 seconds as illustrated in Fig. 16.

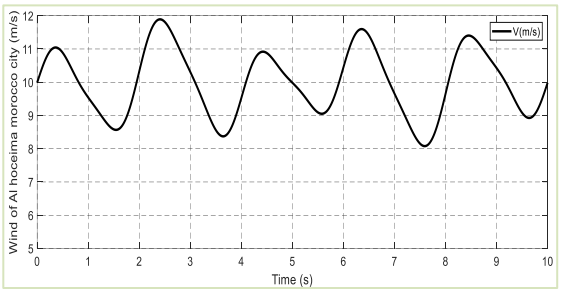

Fig. 16. Wind profile for the referral tracking test

The rotor speed in Fig. 17 provides important information on how wind affects the system's rotational behaviour. The graphic clearly illustrates the dynamic nature of the rotor speed by showing its behaviour over time.

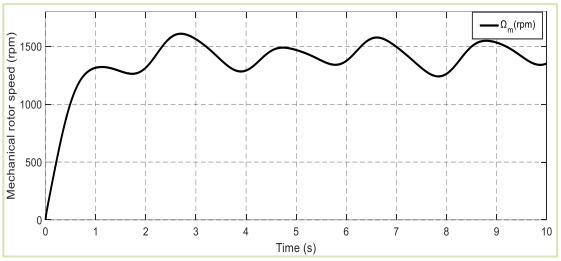

Fig. 17. Mechanical rotor speed (rpm)

As can be seen in Fig. 18(a) and Fig. 18(b), there is a notable convergence of the active and reactive power towards their references. It is noteworthy that a mere fluctuation in wind speed can result in a significant variance in the extracted active power, which can vary from 550W to 1500W. It is evident that the active power (Ps) increases with increasing wind speed and falls with decreasing wind speed. On the grid side, a unit power factor is ensured by maintaining the reference value for reactive power at zero.

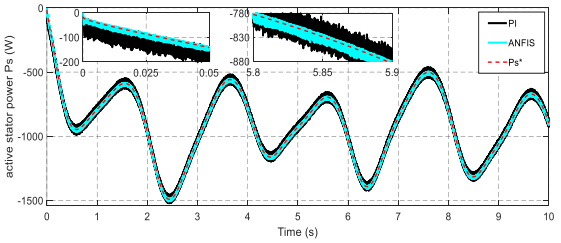

(a) Active power

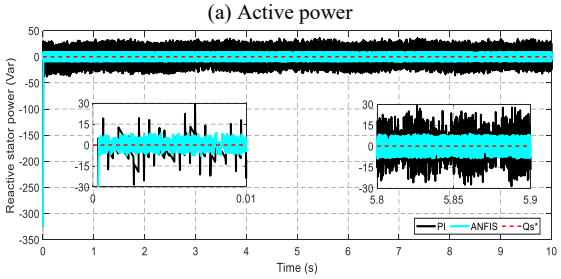

(b) Reactive power

Fig. 18. Active and reactive stator power under random wind test

The data in Fig. 19 (a), (b), (c), and (d) demonstrate how the rotor currents, stator currents and the wind speed, correlate with each other. The effect of wind variation on the stator and rotor current magnitudes is amply illustrated by these data. Interestingly, the currents show a maximum value of 4A for each, which denotes the highest possible electrical flow levels in the system. This reliance on the wind profile emphasizes how important external environmental elements are in influencing how well the system operates.

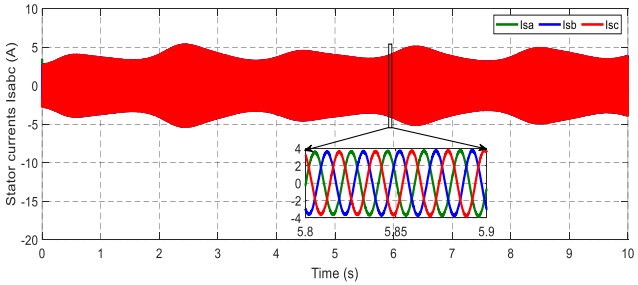

(a) Stator I_{sabc} observed under the PI case of random wind

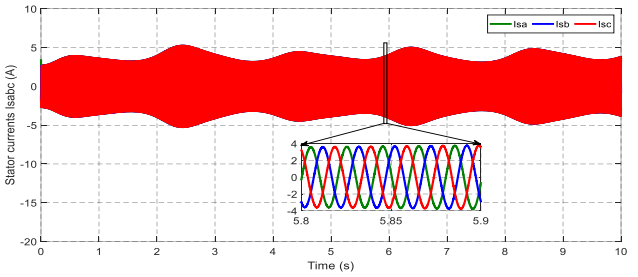

(b) Stator I_{sabc} observed under the ANFIS case of random wind

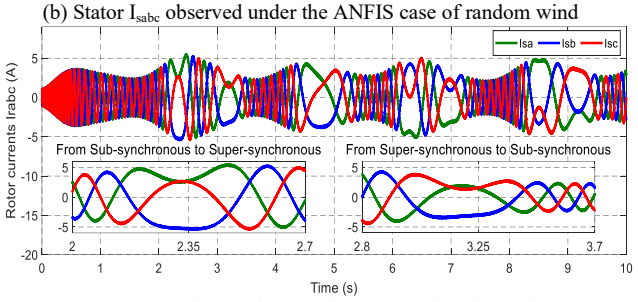

(c) Rotor I_{rabc} observed under the PI case of random wind

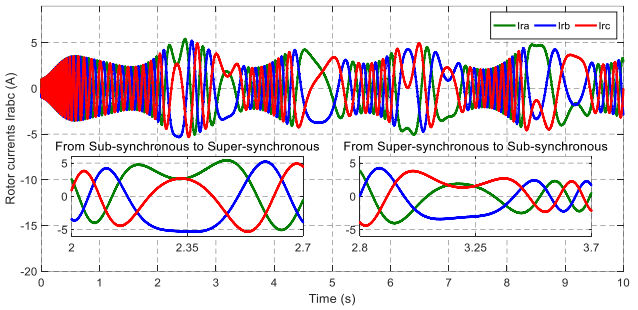

(d) Rotor I_{rabc} observed under the ANFIS case of random wind

Fig. 19. Stator and Rotor currents PI and ANFIS controllers' case random wind

The power factor of the system is shown graphically in Fig. 20, where it is about equal to 1. There are also fluctuations on the plot, which are related to the way the system works and the variations in wind speed.

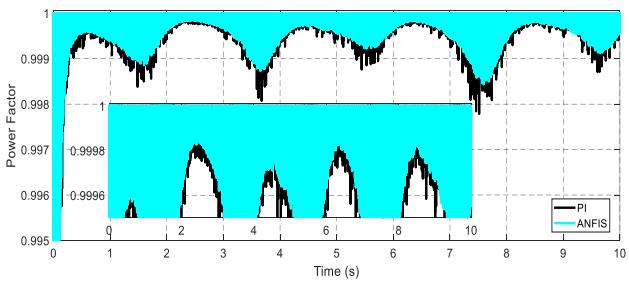

Fig. 20. Power Factor case random wind

In Fig. 21, the net improvement in THD of the current generated by employing the two techniques is visually represented. The data presented offers valuable insights into the effectiveness of these methods in enhancing the purity and efficiency of the current waveform, providing a quantitative measure of the improvements achieved.

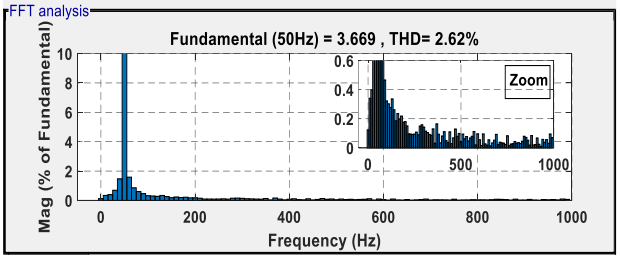

Fig. 21. Total improvement in THD of the current generated by combining the two techniques

TABLE II. COMPARING RESULTS WITH LITERATURE'S REFERENCE CONTROL STRATEGIES

References	Strategies	THD (%)
[36]	DPC control using L-filter	10.79
	DPC control using LCL-filter	4.05
[37]	Second order SMC	3.13
[38]	Integral SMC	9.7
	Multi-resonant-based SMC	3.2
[39]	Virtual flux DPC	4.2
	DPC	4.9
Proposed strategy	IVC based on ANFIS	2.62

In order to demonstrate the results of the proposed IVC-ANFIS, it is essential to compare it with other techniques in the literature. However, it should be noted that it is rare to find similar studies carried out under the same conditions. This limits the possibility of comparison. According to Table II, the proposed IVC-ANFIS using ANFIS controllers shows a higher efficiency in THD reduction compared to other controllers used in the literature. Overall, the results show the performance of the proposed control approach in achieving accurate, robust, and fast response control while reducing internal and external disturbances.

VI. CONCLUSION

This paper presents an Adaptive Neuro-Fuzzy Inference System (ANFIS) controller-based indirect vector control (IVC) method for a doubly fed induction generator (DFIG) and compares its performance with a proportional-integral (PI) controller. According to the simulation results, the suggested ANFIS-based method outperforms the IVC-PI controller and performs better under comparable operating conditions. Furthermore, while using IVC-ANFIS control instead of IVC-PI control, the stator current's Total Harmonic Distortion (THD) is significantly decreased. Furthermore, the ANFIS controller efficiently controls both active and reactive power by modifying generator torque and speed according to the wind speed variation. These results highlight the effectiveness and resilience of the artificial intelligence-based indirect vector control method for DFIG systems for Wind Energy Conversion Systems (WECS). Moreover, it has been demonstrated that the application of IVC-ANFIS control results in improved turbine lifespan, increased monitoring system dependability, and favourable technical, financial, and environmental performance outcomes.

REFERENCES

[1] C. Dardabi *et al*., "Enhancing the control of doubly fed induction generators using artificial neural networks in the presence of real wind profiles," *PLoS ONE*, vol. 19, no. 4, p. e0300527, 2024.

[2] H. Chojaa *et al*., "Robust Control of DFIG-Based WECS Integrating an Energy Storage System With Intelligent MPPT Under a Real Wind Profile," *IEEE Access*, vol. 11, pp. 90065–90083, 2023.

[3] L. Li *et al*., "Review and outlook on the international renewable energy development," *Energy and Built Environment*, vol. 3, no. 2, pp. 139–157, Apr. 2022, doi: 10.1016/j.enbenv.2020.12.002.

[4] A. Çiçek and O. Erdinç, "Risk-averse optimal bidding strategy considering bi-level approach for a renewable energy portfolio manager including EV parking lots for imbalance mitigation," *Sustainable Energy, Grids and Networks*, vol. 28, p. 100539, 2021.

[5] M. A. Mossa, T. Duc Do, A. Saad Al-Sumaiti, N. V. Quynh, and A. A. Z. Diab, "Effective Model Pr dictive Voltage Control for a Sensorless Doubly Fed Induction Generator," *IEEE Canadian Journal of Electrical and Computer Engineering*, vol. 44, no. 1, pp. 50–64, 2021.

[6] A. H. Besheer, X. Liu, S. Fathalla, M. Rabah, A. Mahgoub, and H. Rashad, "Overview on fast primary frequency adjustment technology for wind power future low inertia systems," *Alexandria Eng. J*., vol. 78, pp. 318–338, 2023, doi: 10.1016/j.aej.2023.07.032.

[7] S. L. S. Louarem, D. E. C. Belkhiat, T. Bouktir, and S. Belkhiat, "An Efficient Active and Reactive Power Control of DFIG for a Wind Power Generator," *Eng. Technol. Appl. Sci. Res*., vol. 9, no. 5, pp. 4775–4782, Oct. 2019.

[8] M. A. Mossa, M. K. Abdelhamid, A. A. Hassan, and N. Bianchi, "Improving the Dynamic Performance of a Variable Speed DFIG for Energy Conversion Purposes Using an Effective Control System," *Processes*, vol. 10, no. 3, p. 456, 2022.

[9] E. Chetouani, Y. Errami, A. Obbadi, and S. Sahnoun, "Self-adapting PI controller for grid-connected DFIG wind turbines based on recurrent neural network optimization control under unbalanced grid faults," *Electric Power Systems Research*, vol. 214, p. 108829, Jan. 2023.

[10] A. Mansouri, A. El Magri, R. Lajouad, I. El Myasse, Y. El Khlifi, and F. Giri, "Wind energy based conversion topologies and maximum power point tracking: A comprehensive review and analysis," *e-Prime - Advances in Electrical Engineering, Electronics and Energy*, vol. 6, p. 100351, 2023.

[11] M. A. Mossa, H. Echeikh, and A. Iqbal, "Enhanced control technique for a sensor-less wind driven doubly fed induction generator for energy conversion purpose," *Energy Reports*, vol. 7, pp. 5815–5833, 2021.

[12] A. Çiçek and O. Erdinç, "Optimal Bidding Strategy Considering Bilevel Approach and Multistage Process for a Renewable Energy Portfolio Manager Managing RESs with ESS," in *IEEE Systems Journal*, vol. 16, no. 4, pp. 6062-6073, Dec. 2022.

[13] A. K. Mohapatra, S. Mohapatra, A. Patnaik, and P. C. Sahu, "Design and modelling of an AI governed type-2 Fuzzy tilt control strategy for AGC of a multi-source power grid in constraint to optimal dispatch," *e-Prime - Advances in Electrical Engineering, Electronics and Energy*, vol. 7, p. 100487, 2024.

[14] S. Karupusamy *et al*., "Torque control-based induction motor speed control using Anticipating Power Impulse Technique," *The International Journal of Advanced Manufacturing Technology*, pp. 1-9, 2023, doi: 10.1007/s00170-023-10893-5.

[15] A. Guediri, A. Guediri, and S. Touil, "Modeling and Comparison of Fuzzy-PI and Genetic Control Algorithms for Active and Reactive Power Flow between the Stator (DFIG) and the Grid," *Eng. Technol. Appl. Sci. Res.*, vol. 12, no. 3, pp. 8640–8645, Jun. 2022.

[16] M. Chahboun and H. Hihi, "Robust Control of a Wind Power System Based on a Doubly-Fed Induction Generator Using a Fuzzy Controller," *Lecture Notes in Networks and Systems*, pp. 724–734, 2023, doi: 10.1007/978-3-031-29857-8_72.

[17] B. Desalegn, D. Gebeyehu, and B. Tamrat, "Evaluating the performances of PI controller (2DOF) under linear and nonlinear operations of DFIG-based WECS: A simulation study," *Heliyon*, vol. 8, no. 12, p. e11912, Dec. 2022, doi: 10.1016/j.heliyon. 2022.e11912.

[18] B. Srinu Naik, “Comparison of Direct and Indirect Vector Control of Induction Motor,” *Int. J. New Technol. Sci. Eng*., vol. 1, no. 1, pp. 110–131, 2014.

[19] I. Griche, S. Messalti, K. Saoudi, and M. Y. Touafek, “A new adaptive neuro-fuzzy inference system (ANFIS) and PI controller to voltage regulation of power system equipped by wind turbine,” *Eur. J. Electr. Eng.*, vol. 21, no. 2, pp. 149–155, 2019, doi: 10.18280/ejee.210204.

[20] M. Almaged, A. Mahmood, and Y. H. S. Alnema, “Design of an Integral Fuzzy Logic Controller for a Variable-Speed Wind Turbine Model,” *J. Robot. Control*, vol. 4, no. 6, pp. 762–768, 2023, doi: 10.18196/jrc.v4i6.20194.àpp

[21] R. T. Kumar and C. C. A. Rajan, "Integration of hybrid PV-wind system for electric vehicle charging: Towards a sustainable future," *e-Prime - Advances in Electrical Engineering, Electronics and Energy*, vol. 6, p. 100347, 2023.

[22] A. A. Eshkaftaki, A. Rabiee, A. Kargar, and S. T. Boroujeni, “An Applicable Method to Improve Transient and Dynamic Performance of Power System Equipped With DFIG-Based Wind Turbines,” *IEEE Transactions on Power Systems*, vol. 35, no. 3, pp. 2351–2361, 2020.

[23] D. N. Truong and V. T. Bui, “Hybrid PSO-optimized ANFIS-based model to improve dynamic voltage stability,” *Engineering, Technology & Applied Science Research*, vol. 9, no. 4, pp. 4384-4388, 2019.

[24] A. Khajeh, H. Torabi, and Z. S. Siahkaldeh, “ANFIS based sliding mode control of a DFIG wind turbine excited by an indirect matrix converter,” *International Journal of Power Electronics and Drive Systems (IJPEDS)*, vol. 14, no. 3, pp. 1739–1747, Sep. 2023.

[25] M. S. Arifin, M. N. Uddin and W. Wang, "Neuro-Fuzzy Adaptive Direct Torque and Flux Control of a Grid Connected DFIG-WECS with Improved Dynamic Performance," *2022 IEEE Industry Applications Society Annual Meeting (IAS)*, pp. 1-8, 2022.

[26] A. Ranjan, D. V. Bhaskar and V. L. Srinivas, "A Novel Control Approach for Grid-Integrated DFIG Driven Wind Energy Systems," *2023 IEEE IAS Global Conference on Emerging Technologies (GlobConET)*, pp. 1-6, 2023.

[27] M. A. Mossa, H. Echeikh, N. V. Quynh, and N. Bianchi, “Performance dynamics improvement of a hybrid wind/fuel cell/battery system for standalone operation,” *IET Renew. Power Gener*., vol. 17, no. 2, pp. 349-375, 2022.

[28] X. Zhu, Y. Wang, L. Xu, X. Zhang, and H. Li, "Virtual inertia control of DFIG-based wind turbines for dynamic grid frequency support," *IET Conference on Renewable Power Generation (RPG 2011)*, pp. 1-6, 2011, doi: 10.1049/cp.2011.0189.

[29] M. A. Mossa, O. Gam, and N. Bianchi, "Dynamic performance enhancement of a renewable energy system for grid connection and stand-alone operation with battery storage," *Energies*, vol. 15, no. 3, p. 1002, 2022.

[30] W. Tang, J. Hu, Y. Chang, and F. Liu, "Modeling of DFIG-Based Wind Turbine for Power System Transient Response Analysis in Rotor Speed Control Timescale," in *IEEE Transactions on Power Systems*, vol. 33, no. 6, pp. 6795-6805, Nov. 2018, doi: 10.1109/TPWRS.2018.2827402.

[31] M. A. Mossa, N. E. Ouanjli, O. Gam, and T. D. Do, “Enhancing the Performance of a Renewable Energy System Using a Novel Predictive Control Method,” *Electronics*, vol. 12, p. 3408, 2023.

[32] H. Chojaa, A. Derouich, S. E. Chehaidia, O. Zamzoum, M. Taoussi, and H. Elouatouat, “Integral sliding mode control for DFIG based WECS with MPPT based on artificial neural network under a real wind profile,” *Energy Reports*, vol. 7, pp. 4809–4824, 2021.

[33] H. Jenkal, B. Bossoufi, A. Boulezhar, A. Lilane, and S. Hariss, “Vector control of a doubly fed induction generator wind turbine,” *Mater. Today Proc*., vol. 30, pp. 976–980, 2019.

[34] M. A. Khan, A. Ali, and I.-U.-H. Shaikh, “Hybrid Fuzzy-PI and ANFIS Controller Design for Rotor Current Control of DFIG Based Wind Turbine,” *Pakistan Journal of Engineering and Technology*, vol. 5, no. 1, pp. 35–41, Mar. 2022, doi: 10.51846/vol5iss1pp35-41.

[35] Y. Guo and M. E. A. Mohamed, “Speed Control of Direct Current Motor Using ANFIS Based Hybrid P-I-D Configuration Controller,” *IEEE Access*, vol. 8, pp. 125638–125647, 2020.

[36] Y. Sahri, S. Tamalouzt, F. Hamoudi, S. Lalouni, and M. Bajaj, “New intelligent direct power control of DFIG-based wind conversion system by using machine learning under variations of all operating and compensation modes,” *Energy Reports*, vol. 7, pp. 6394–6412, 2021.

[37] R. K. Behara and A. K. Saha, “Artificial Intelligence Methodologies in Smart Grid-Integrated Doubly Fed Induction Generator Design Optimization and Reliability Assessment: A Review,” *Energies*, vol. 15, no. 19, p. 7164, Sep. 2022, doi: 10.3390/en15197164.

[38] I. K. Amin, M. Nasir Uddin, and M. Marsadek, “ANFIS based Neuro-Fuzzy Control of DFIG for Wind Power Generation in Standalone Mode,” *2019 IEEE International Electric Machines & Drives Conference (IEMDC)*, pp. 2077-2082, 2019.

[39] J. Tavoosi *et al*., “A machine learning approach for active/reactive power control of grid-connected doubly-fed induction generators,” *Ain Shams Eng. J*., vol. 13, no. 2, p. 101564, 2022.

[40] M. M. Alhato and S. Bouallègue, "Direct power control optimization for doubly fed induction generator based wind turbine systems," *Math. Comput. Appl*., vol. 24, no. 3, p. 77, 2019, doi:10.3390/mca24030077.

[41] A. Yahdou, "Second order sliding mode control of a dual-rotor wind turbine system by employing a matrix converter," *J. Electr. Eng.*, vol. 16, no. 3, 2017.

[42] Y. Quan, L. Hang, Y. He, and Y. Zhang, "Multi-resonant-based sliding mode control of DFIG-based wind system under unbalanced and harmonic network conditions," *Appl. Sci.*, vol. 9, no. 6, p. 1124, 2019.

[43] N. A. Yusoff, A. M. Razali, K. A. Karim, T. Sutikno, and A. Jidin, "A concept of virtual-flux direct power control of three-phase AC–DC converter," *Int. J. Power Electron. Drive Syst*., vol. 8, no. 4, pp. 1776-1784, 2017.